Alternative Sites for Proton Entry from the Cytoplasm to the Quinone Binding Site in *Escherichia coli* Succinate Dehydrogenase†

Victor W. T. Cheng, Antonia Johnson, Richard A. Rothery, and Joel H. Weiner*

Membrane Protein Research Group, Department of Biochemistry, University of Alberta, 473 Medical Sciences Building, Edmonton, Alberta T6G 2H7, Canada

Received May 28, 2008; Revised Manuscript Received July 7, 2008

ABSTRACT: *Escherichia coli* succinate dehydrogenase (Sdh) belongs to the highly conserved complex II family of enzymes that reduce ubiquinone. These enzymes do not generate a protonmotive force during catalysis and are electroneutral. Because of its electroneutrality, the quinone reduction reaction must consume cytoplasmic protons which are released stoichiometrically during succinate oxidation. The X-ray crystal structure of *E. coli* Sdh shows that residues SdhB^{G227}, SdhC^{D95}, and SdhC^{E101} are located at or near the entrance of a water channel that has been proposed to function as a proton wire connecting the cytoplasm to the quinone binding site. However, the pig and chicken Sdh enzymes show an alternative entrance to the water channel via the conserved SdhD^{Q78} residue. In this study, site-directed mutants of these four residues were created and characterized by *in vivo* growth assays, *in vitro* activity assays, and electron paramagnetic resonance spectroscopy. We show that the observed water channel in the *E. coli* Sdh structure is the functional proton wire *in vivo*, while *in vitro* results indicate an alternative entrance for protons. *In silico* examination of the *E. coli* Sdh reveals a possible H-bonding network leading from the cytoplasm to the quinone binding site that involves SdhD^{D15}. On the basis of these results we propose an alternative proton pathway in *E. coli* Sdh that might be functional only *in vitro*.

The mitochondrial respiratory chain contains a complex electron relay system that converts chemical energy into a transmembrane electrochemical proton gradient. Complexes I, III, and IV have been studied extensively and are known to translocate protons through either vectorial or scalar mechanisms. Complex II, commonly known as succinate: quinone oxidoreductase (SQR) or succinate dehydrogenase (Sdh),[1] is the sole enzyme of the mitochondrial respiratory chain that is electroneutral. *Escherichia coli* possesses an Sdh that is essentially identical in structure and function to its mitochondrial counterpart (*1*−*3*) and represents an excellent model system for studying complex II enzymes.

The physiological function of Sdh is to couple succinate oxidation to ubiquinone reduction and is achieved by using five unique cofactors that are assembled in the holoenzyme. In SdhA, a covalently attached flavin adenine dinucleotide (FAD) molecule is present to catalyze succinate oxidation by a hydride transfer mechanism (*4, 5*). Electrons are then shuttled singly through the electron transfer subunit (SdhB) which comprises a [2Fe-2S], a [4Fe-4S], and a [3Fe-4S] cluster. Residues from the membrane anchor domain (SdhCD) and SdhB converge to form the quinone binding site (a Q_P-site, proximal to SdhB/FrdB) wherein ubiquinone (UQ) is reduced to ubiquinol (UQH_2). Sandwiched between SdhC and SdhD is a heme *b* molecule that is not essential to enzyme function (*6*).

Complex II enzymes have evolved with two basic overall architectures. The first is represented by the archetypical mitochondrial type enzyme that comprises a catalytic dimer (SdhAB) that is anchored to the matrix side of the membrane by two hydrophobic subunits (SdhCD). In *E. coli* and other bacteria such as *Paracoccus denitrificans*, the SdhCD subunits anchor SdhAB to the inner surface of the cytoplasmic membrane. An important subclass of complex II enzymes is represented by the heterotrimeric succinate dehydrogenase of *Bacillus subtilis* and the fumarate reductase of *Wolinella succinogenes*. These differ from the archetypical complex II in that they have only one membrane anchor subunit wherein two *b*-type hemes are integrated to provide an electron transfer relay to a periplasmically oriented quinone binding site (a Q_D-site, distal to SdhB/FrdB). In the case of the true Complex II archetypes, just a single heme *b* moiety is incorporated into the membrane anchor and only the Q_P-site is functional. The presence of a Q_D-site has been observed in the homologous fumarate reductase enzyme from *E. coli*, but its function remains controversial in mitochondrial and *E. coli* Sdh (*2, 7*−*10*).

† This work was funded by the Canadian Institutes of Health Research. Infrastructure funding was provided by the Canada Foundation for Innovation. V.W.T.C. was supported by an Alberta Heritage Foundation for Medical Research Graduate Studentship. J.H.W. holds a Canada Research Chair in Membrane Biochemistry.

* To whom correspondence should be addressed. Tel: (780) 492-2761. Fax: (780) 492-0886. E-mail: joel.weiner@ualberta.ca.

[1] Abbreviations: E_m, midpoint potential; [Fe-S], iron−sulfur; FAD, flavin adenine dinucleotide; EPR, electron paramagnetic resonance; G-F, glycerol−fumarate; H-bond, hydrogen bond; KIE, kinetic isotope effect; MTT, 2-(4,5-dimethyl-2-thiazolyl)-3,5-diphenyl-2*H*-tetrazolium bromide; PMS, phenazine methosulfate; Q_P-site, quinone binding site proximal to SdhB/FrdB; Q_D-site, quinone binding site distal to SdhB/FrdB; Sdh, *Escherichia coli* succinate dehydrogenase; SDS−PAGE, sodium dodecyl sulfate−polyacrylamide gel electrophoresis; UQ/UQH_2, ubiquinone/ubiquinol; WT, wild-type.

10.1021/bi801008e CCC: $40.75
Published on Web 08/09/2008

Because of the differences in subunit, heme, and Q-site compositions in the complex II superfamily, proton movement during quinone oxidation/reduction is extremely diverse. The *E. coli* and mitochondrial Sdh enzymes do not generate a protonmotive force during catalysis as the two cytoplasmic protons consumed by quinone reduction are supplied by the succinate oxidation reaction. However, in Gram-positive bacteria such as *Bacillus* sp., a heterotrimeric Sdh has been shown to be electrogenic when functioning as a quinol:fumarate oxidoreductase (*11*), and its succinate:quinone oxidoreductase activity is dependent on the transmembrane potential (*12, 13*). The *W. succinogenes* fumarate reductase catalyzes an electroneutral reaction that involves a scalar movement of protons across the membrane that is canceled by a stoichiometric vectorial movement of protons (*14, 15*).

X-ray crystal structures of Sdh have been obtained for the *E. coli*, chicken, and pig enzymes (*1*−*3, 16*), and this has led to a better understanding of succinate oxidation versus fumarate reduction at the flavin active site (*5, 17*), electron transfer through the iron−sulfur clusters (*18*−*20*), ubiquinone binding and reduction (*16, 21*), the role of heme in enzyme assembly and function (*6, 22*), and its generation of reactive oxygen species (*23, 24*). The reduction of ubiquinone to ubiquinol requires protons at the quinone binding site, and very little biochemical data are available on how protons are shuttled from the cytoplasm to this Q_P-site. This information is required for a detailed mechanism of enzyme catalysis and may even be crucial to understanding how certain disease states are manifested through mutations in complex II. Disease phenotypes associated with Sdh include Leigh syndrome (*25, 26*), Kearns−Sayre syndrome (*27*), and abnormal muscular development (*28, 29*), as well as familial pheochromocytoma and paraganglioma (*30*).

Crystallographic evidence supporting the existence of a conserved water-filled proton channel leading from the cytoplasm to the Q_P-site is not obvious in the three available structures of tetrameric Sdh as there is a high degree of variation in the location of water molecules. A potential proton wire in the form of a water channel is observed in the *E. coli* structure (*1, 16*), and we set out to determine whether the observed channel is crucial for enzyme function using a site-directed mutagenesis approach.

EXPERIMENTAL PROCEDURES

Bacterial Strains and Plasmids. E. coli strain DW35 (Δ*frdABCD*, *sdhC::kan*) (*31*) was used for all enzyme expression and growth studies. Expression of wild-type and mutant Sdh was anaerobically induced by using the plasmid pFAS, which encodes the *Sdh* operon under the control of the *frd* promoter (*32*). Laboratory strain TG1 (*supE hsd*Δ5 *thi* Δ(*lac-proAB*) *F*′[*traD*36 *proAB*$^+$ *lacI*^{q} *lacZ*ΔM15]; GE Healthcare) and plasmid pTZ18R (Amp^R*lacZ*′; GE Healthcare) were used for molecular cloning and mutagenesis.

Cloning. The 3.7 kb *Kpn*I−*Sph*I fragment of pFAS was subcloned into pTZ18R, and this recombinant plasmid was used as the template for site-directed mutagenesis (*20*). Sdh mutants were constructed using mutagenic oligonucleotides (Sigma), *Dpn*I (Invitrogen), and Pfu DNA polymerase (Fermentas) in accordance to the QuikChange protocol (Stratagene). Mutants were verified by DNA sequencing (DNA Core Facility, Department of Biochemistry, University of Alberta) and cloned back into the pFAS expression vector. The mutant plasmids were then transformed into DW35 for biochemical studies. Preparation of competent cells and transformations of plasmids into competent cells were carried out as described in ref *33*.

Enzyme Expression and Preparation. Wild-type and mutant enzymes were expressed in DW35 cells, and isolated membranes enriched in Sdh were prepared by French pressure lysis followed by differential ultracentrifugation (*20*). All final membrane preparations containing activated enzymes were suspended in 100 mM MOPS/5 mM EDTA/1 mM malonate at pH 7.

Growth Assays. Aerobic growth on succinate and anaerobic growth on glycerol−fumarate were carried out as previously described (*20, 34*). A Klett−Summerson colorimeter equipped with a no. 6 filter was used to monitor bacterial growth.

SDS−*PAGE.* Protein concentrations were estimated by the Lowry method (*35*) with the inclusion of 1% (w/v) sodium dodecyl sulfate in the mixture (*36*). Protein (30 μg) was resolved on a 12% SDS−PAGE gel (*33*) and visualized by Coomassie blue staining. Low molecular mass markers from Bio-Rad include phosphorylase *b* (97.4 kDa), bovine serum albumin (66.2 kDa), ovalbumin (45.0 kDa), carbonic anhydrase (31.0 kDa), soybean trypsin inhibitor (21.5 kDa), and lysozyme (14.4 kDa).

Flavin Quantification. Fluorometric quantification of the covalent flavin of Sdh was carried out in triplicate as described (*37*), using 5 mg of protein as starting material.

Enzyme Assays. Succinate-dependent reduction of 2-(4,5-dimethyl-2-thiazolyl)-3,5-diphenyl-2*H*-tetrazolium bromide (MTT, $\epsilon = 17\ mM^{-1}\ cm^{-1}$) was measured spectrophotometrically at 570 nm in the presence of 750 μM phenazine methosulfate (PMS) and 0.1% Triton X-100 (*38*). Succinate-dependent reduction of Q_0 ($\epsilon = 0.73\ mM^{-1}cm^{-1}$) and fumarate-dependent oxidation of plumbagin ($\epsilon = 3.95\ mM^{-1}\ cm^{-1}$) were monitored at 410 and 419 nm, respectively. Turnover numbers were calculated based on covalent flavin (SdhA) concentrations. All assays were carried out using isolated membranes enriched in Sdh.

Redox Titration and EPR Spectroscopy. Redox titrations were carried out anaerobically under argon at 25 °C on Sdh-enriched membranes at a total protein concentration of approximately 30 mg mL^{-1} in 100 mM MOPS/5 mM EDTA (pH 7.0). The following redox mediators were used at a concentration of 25 μM: 2,6-dichloroindophenol, 1,2-naphthoquinone, toluylene blue, phenazine methosulfate, thionine, methylene blue, resorufin, indigotrisulfonate, indigocarmine, anthraquinone-2-sulfonic acid, and neutral red. EPR spectra were recorded using a Bruker Elexsys E500 EPR spectrometer equipped with an Oxford Instruments ESR900 flowing helium cryostat. Spectra of the [3Fe-4S] cluster were determined at 12 K while that of heme *b* were determined at 9 K, both at a microwave power of 20 mW and a frequency of 9.38 GHz. All spectra were corrected for internal EPR tube diameters. Presented data were gathered from two potentiometric titrations for each Sdh mutant, once via reduction by dithionite and once via oxidation by ferricyanide.

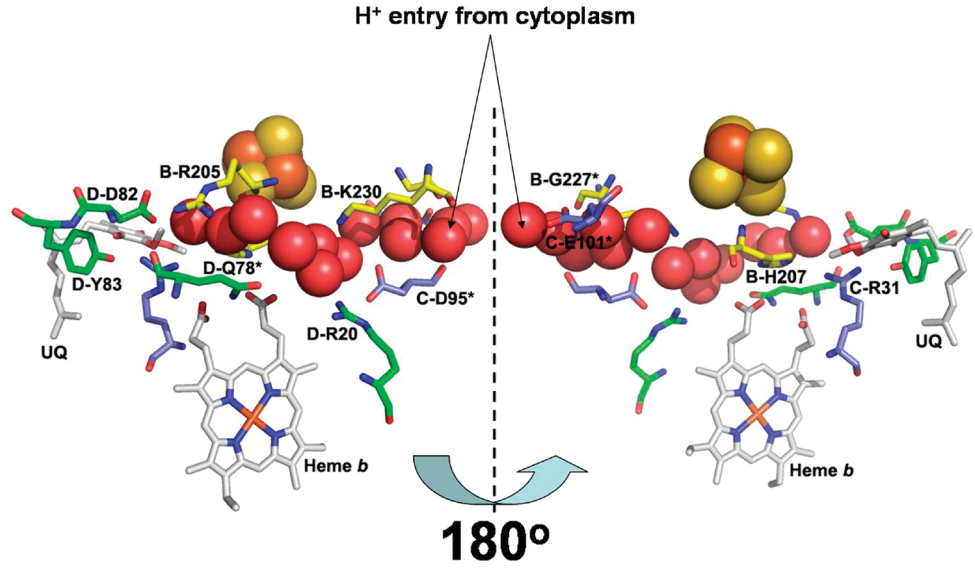

FIGURE 1: Two views of the putative water channel in *E. coli* Sdh leading from the cytoplasm to the Q-site. Protons required for ubiquinone reduction are acquired from the cytoplasm via this proposed water channel. Residues from SdhB, SdhC, and SdhD interact with this channel, which passes near the [3Fe-4S] cluster and the heme *b*. Residues that are examined in this study are marked by an asterisk. Also shown are residues SdhC^{R31}, SdhD^{D82}, and SdhD^{Y83}, which have been implicated in the ubiquinone binding and reduction mechanism (*16, 21*). The figure was generated from PDB file 1NEK using PyMOL v.0.99 (DeLano Scientific LLC.).

Table 1: List of Residues Studied by Site-Directed Mutagenesis[a]

residue	conservation	mutation	predicted effect on putative water channel
SdhB-G227	similar	G → L	adds hydrophobic bulk; blocks water channel entrance
SdhC-D95	yes	D → E	extends side chain and alters H-bonding network
		D → L	eliminates potential H-bond to water channel
SdhC-E101	no	E → D	shortens side chain and alters H-bonding network
		E → L	eliminates potential H-bond to water channel
SdhD-Q78	yes	Q → L	eliminates potential H-bond to water channel

[a] ClustalW alignments with Sdh from human, pig, cow, and chicken were performed, and the conservation of the residue is indicated. The mutation made at each position, as well as its rationale, is also listed.

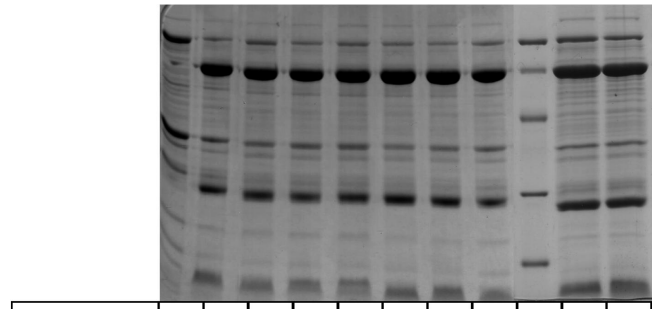

FIGURE 2: Assembly of mutant Sdh enzymes. Thirty micrograms of membrane proteins was separated on a 12% SDS−polyacrylamide gel and stained by Coomassie blue. The concentrations of covalent flavin, determined as described in Experimental Procedures, in each enzyme preparation are also shown. ND: not determined.

RESULTS

Inspection of the *E. coli* Sdh crystal structure (PDB file 1NEK) (*1*) reveals a putative water channel leading from the cytoplasm to the Q_P-site (*10, 16*). Residues which line this water channel (<4Å away) are highlighted in Figure 1 wherein residues examined in this study are marked by asterisks. A list of mutants generated by site-directed mutagenesis is shown in Table 1, along with their predicted effects on the water channel as well as the conservation of the residue in the Sdh family.

A Coomassie blue-stained SDS−PAGE gel (Figure 2) shows that all Sdh mutant enzymes correctly assemble to the cytoplasmic membrane, and Sdh expression levels, quantitated by covalent flavin content, correlate with the amount of protein detected.

The ability of the mutant Sdh enzymes to complement *E. coli* DW35 *in vivo* was examined using plasmid-mediated high level expression of the *sdh* operon. Figure 3A shows that all Sdh mutant enzymes were able to complement DW35 and support aerobic growth on succinate minimal medium at essentially the same growth rate and growth density even though enzyme expression was induced by the anaerobic *frd* promoter. Since Sdh can readily function as a fumarate reductase under anaerobic conditions (*32*), we also tested the ability of the mutant enzymes to support anaerobic growth on glycerol−fumarate (G-F) medium. As expected, *E. coli* DW35 itself cannot grow on G-F minimal medium but can readily do so when transformed with the pFAS plasmid expressing wild-type (WT) Sdh (Figure 3B). Unlike the results seen for aerobic growth on succinate, the mutant enzymes displayed varying abilities to complement the deletion strain for growth on G-F. In particular, the single mutants SdhC^{D95L}DAB and SdhCDAB^{G227L} and the double mutants containing the latter substitution (SdhC^{D95E}DAB^{G227L} and SdhC^{D95L}DAB^{G227L}) exhibited severely depressed growth.

The steady-state succinate:PMS/MTT assay is a nonphysiological assay that measures succinate oxidase activity

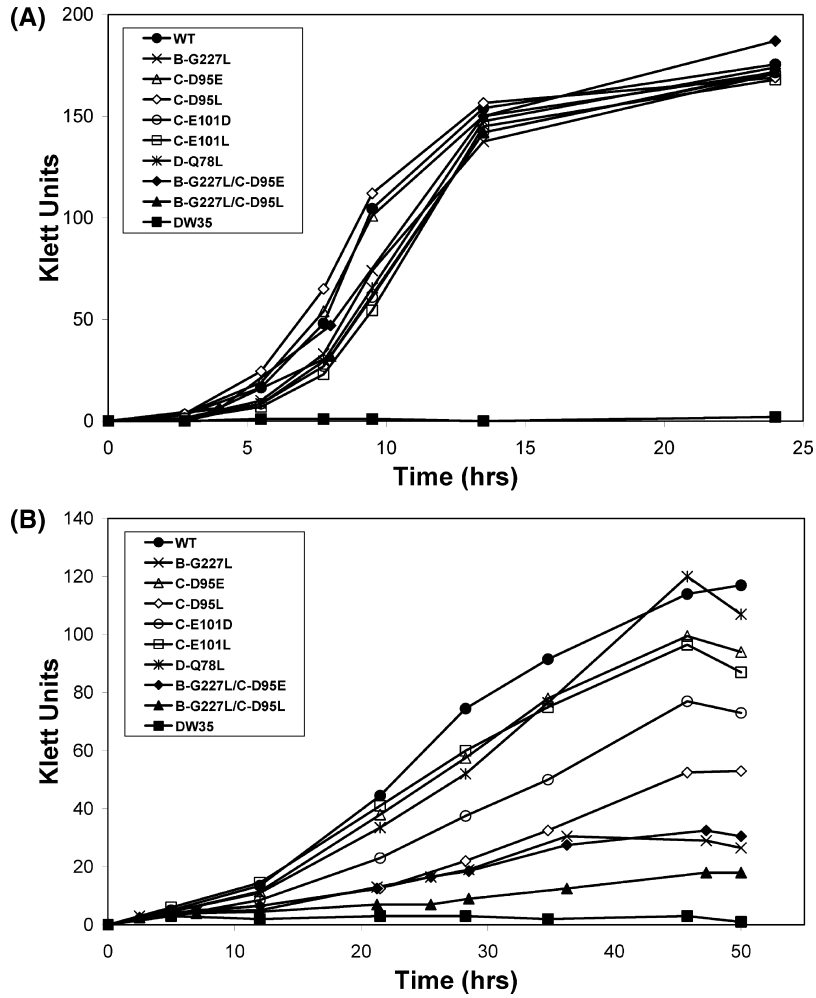

FIGURE 3: Growth of *E. coli* DW35 with and without expression of wild-type and mutant Sdh enzymes. (A) Aerobic growth on succinate minimal medium. 25 mL cultures in 125 mL sidearm flasks were grown at 37 °C with shaking. (B) Anaerobic growth on glycerol−fumarate minimal medium. 125 mL sidearm flasks filled with bacterial culture were grown at 37 °C with magnetic stirring. Growth curves are representative of triplicate experiments wherein cell density measurements (Klett units) were collected from two separate and independent bacterial cultures at the times indicated.

Table 2: Succinate-Dependent Reduction of PMS/MTT by Mutant Enzymes at pH 7, pH 8, and pD 7.4[a]

	turnover (s^{-1})		
	pH 7	pH 8	pD 7.4
WT Sdh	11.5 ± 0.4	20.9 ± 1.8	7.5 ± 0.7
B-G227L	9.3 ± 0.2	15.9 ± 1.8	6.4 ± 0.4
C-D95E	15.6 ± 0.4	29.6 ± 2.8	10.6 ± 0.4
C-D95L	10.5 ± 0.3	17.4 ± 0.8	6.7 ± 0.5
C-E101D	9.8 ± 0.3	18.0 ± 0.8	6.0 ± 0.2
C-E101L	8.1 ± 0.7	12.6 ± 0.6	5.3 ± 0.1
D-Q78L	9.9 ± 0.6	20.8 ± 0.3	6.0 ± 0.2
B-G227L/C-D95E	19.9 ± 1.6	ND	ND
B-G227L/C-D95L	9.4 ± 0.9	ND	ND

[a] Succinate was used as electron donor, and reduction of MTT was measured in the presence of 750 μM PMS. Turnover numbers were calculated based on the amount of covalent FAD determined. Triplicate readings were taken at each condition.

independent of Q_P-site functionality. All membrane preparations containing the Sdh mutants, with the exception of $SdhC^{D95E}DAB$, had comparable succinate:PMS/MTT activity relative to the WT enzyme at pH 7, at pH 8, and in deuterium oxide (Table 2), indicating proper assembly and activation of the enzymes. Interestingly, the $SdhC^{D95E}DAB$ mutant had a succinate:PMS/MTT turnover rate that was approximately 50% higher than the WT enzyme at all three conditions. The succinate:Q_0 (succinate oxidation coupled to Q_0 reduction) and plumbagin:fumarate (plumbagin oxidation coupled to fumarate reduction) enzyme assays measure physiological and reverse activities of Sdh, respectively. At pH 7, WT Sdh catalyzed Q_0 reduction at a rate of 28 s^{-1} and plumbagin oxidation at a rate of 31 s^{-1}, whereas the mutant enzymes had slower rates of catalysis for both reactions (Tables 3 and 4). The double mutant $SdhC^{D95E}DAB^{G227L}$ also had slower rates of catalysis, but the $SdhC^{D95L}DAB^{G227L}$ construct had wild-type kinetic parameters for succinate:Q_0 activity and remained impaired in the plumbagin:fumarate assay, resulting in a significantly higher Q_0/plumbagin activity ratio at pH 7 (p-value <0.001).

To further assess the functional efficiencies of the proton channel mutant enzymes, the assays were repeated at pH 8 where the H^+ concentration is decreased by 90%. At pH 8, the succinate:Q_0 and plumbagin:fumarate activities of the WT enzyme were determined to be 38 and 16 s^{-1}, respectively, and are compromised in the proton channel mutants. The higher Q_0 reduction and lower plumbagin oxidation activities observed at pH 8 are consistent with previously published results (*5, 39*). Worthy of note is the $SdhCDAB^{G227L}$ mutant which had similar turnover rates of Q_0 reduction and plumbagin oxidation. This contrasts to the other mutants, as

Table 3: Succinate-Dependent Reduction of Q_0 by Mutant Enzymes[a]

	turnover (s^{-1})		K_m (mM)		k_{cat}/K_m (s^{-1} mM^{-1})	
	pH 7	pH 8	pH 7	pH 8	pH 7	pH 8
WT Sdh	27.5 ± 1.8	37.9 ± 3.4	0.18 ± 0.01	0.15 ± 0.01	157	248
B-G227L	14.5 ± 0.5	11.6 ± 1.3	0.16 ± 0.01	0.09 ± 0.01	90	127
C-D95E	16.1 ± 0.5	22.3 ± 1.8	0.18 ± 0.02	0.13 ± 0.01	91	173
C-D95L	16.8 ± 0.7	16.2 ± 2.3	0.13 ± 0.01	0.07 ± 0.01	125	246
C-E101D	14.7 ± 0.9	20.9 ± 1.5	0.13 ± 0.02	0.10 ± 0.01	111	207
C-E101L	12.6 ± 0.1	15.6 ± 1.8	0.10 ± 0.02	0.09 ± 0.01	124	168
D-Q78L	15.8 ± 0.1	17.4 ± 3.9	0.19 ± 0.03	0.06 ± 0.01	83	310
B-G227L/C-D95E	18.6 ± 0.6	ND	0.20 ± 0.01	ND	95	ND
B-G227L/C-D95L	24.8 ± 0.4	ND	0.16 ± 0.02	ND	151	ND

[a] Rates of Q_0 reduction were monitored spectrophotometrically at 410 nm and were determined at varying concentrations of the quinone analogue. k_{cat} and K_m values were obtained by plotting $1/v$ against 1/[S] in a double-reciprocal plot using at least eight activity measurements at different Q_0 concentrations and repeated at least once. ND = not determined.

Table 4: Fumarate-Dependent Oxidation of Reduced Plumbagin by Mutant Enzymes[a]

	turnover (s^{-1})		K_m (mM)		k_{cat}/K_m (s^{-1} mM^{-1})	
	pH 7	pH 8	pH 7	pH 8	pH 7	pH 8
WT Sdh	31.1 ± 1.7	15.9 ± 1.4	0.17 ± 0.02	0.17 ± 0.01	179	93
B-G227L	18.0 ± 0.8	9.1 ± 0.5	0.11 ± 0.01	0.13 ± 0.01	162	71
C-D95E	24.3 ± 3.5	12.7 ± 1.3	0.14 ± 0.03	0.19 ± 0.02	176	68
C-D95L	18.0 ± 3.7	8.6 ± 0.2	0.12 ± 0.01	0.16 ± 0.01	153	53
C-E101D	17.1 ± 1.4	10.4 ± 0.3	0.11 ± 0.01	0.14 ± 0.01	159	73
C-E101L	14.9 ± 1.7	7.7 ± 0.4	0.10 ± 0.01	0.11 ± 0.01	152	71
D-Q78L	16.7 ± 0.9	9.3 ± 0.4	0.08 ± 0.01	0.11 ± 0.01	210	85
B-G227L/C-D95E	23.0 ± 3.6	ND	0.128 ± 0.05	ND	179	ND
B-G227L/C-D95L	21.5 ± 0.4	ND	0.124 ± 0.03	ND	173	ND

[a] Rates of plumbagin oxidation were monitored spectrophotometrically at 419 nm and were determined at varying concentrations of the quinone analogue. k_{cat} and K_m values were obtained by plotting $1/v$ against 1/[S] in a double-reciprocal plot using at least eight activity measurements at different Q_0 concentrations and repeated at least once. ND = not determined.

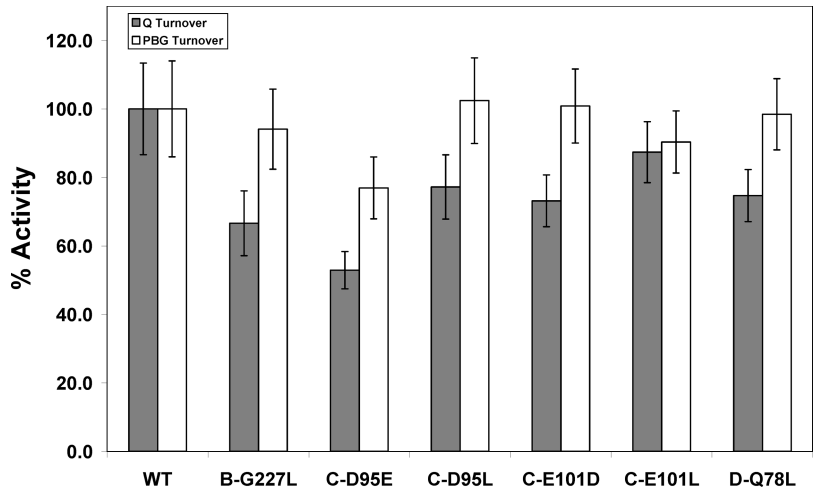

FIGURE 4: Relative enzyme activities in deuterium oxide. Succinate:Q_0 and plumbagin:fumarate oxidoreductase activities were determined at pD 7.4 (measured as pH 7.0 using a pH electrode). 100% activity, as measured from the wild-type Sdh enzyme, corresponds to turnover rates of 10 and 4 s^{-1} for the succinate:Q_0 and plumbagin:fumarate assays, respectively. Q_0 reduction was monitored at a wavelength of 410 nm while plumbagin oxidation was followed at 419 nm. Enzyme activities of each Sdh preparation were gathered from three independent measurements and then normalized against their succinate:PMS/MTT activities.

well as the WT enzyme, which catalyze the forward reaction approximately twice as fast as the reverse reaction at pH 8 (Tables 3 and 4).

We also characterized the abilities of the mutant enzymes to function at pD 7.4 (measured as pH 7 using a pH electrode) in a deuterium oxide solvent. Using D_2O to probe proton transfer reactions and rate-limiting steps in catalytic mechanisms is well established (*40*). The succinate:PMS/MTT, succinate:Q_0, and plumbagin:fumarate activities were determined to be 8, 10, and 4 s^{-1}, respectively, for the WT enzyme at pD 7.4. Figure 4 shows the physiological and reverse enzyme activities of the mutant enzymes relative to WT Sdh while Table 5 presents the results as ratios of comparative activities at pH 7 versus pD 7.4. Only a minor kinetic isotope effect (KIE) was observed in the succinate:PMS/MTT reaction. During Q_0 reduction the mutant enzymes show similar KIE values compared to the WT enzyme (p-value >0.1), but significant differences were observed in the plumbagin oxidation reaction (p-value <0.001). We also observed a general increase in the KIE value for all mutant enzymes as well as the WT enzyme in the plumbagin:fumarate reaction compared to the succinate:Q_0 reaction.

Table 5: Kinetic Isotope Effect on Enzyme Activities[a]

	pH/pD ratio		
	Succ:PMS/MTT	Succ:Q_0	PBG:fumarate
WT Sdh	1.5	2.7	8.1
B-G227L	1.5	2.4	5.8
C-D95E	1.5	2.1	5.8
C-D95L	1.6	2.4	5.1
C-E101D	1.6	2.5	5.5
C-E101L	1.5	2.0	6.0
D-Q78L	1.7	2.6	5.5

[a] Enzymatic activities were measured by using concentrations of Q_0 and plumbagin that are at least 10× their K_m values as determined at pH 7. The pH/pD ratios were determined by dividing the rate of substrate turnover at pH 7 by that obtained at pD 7.4.

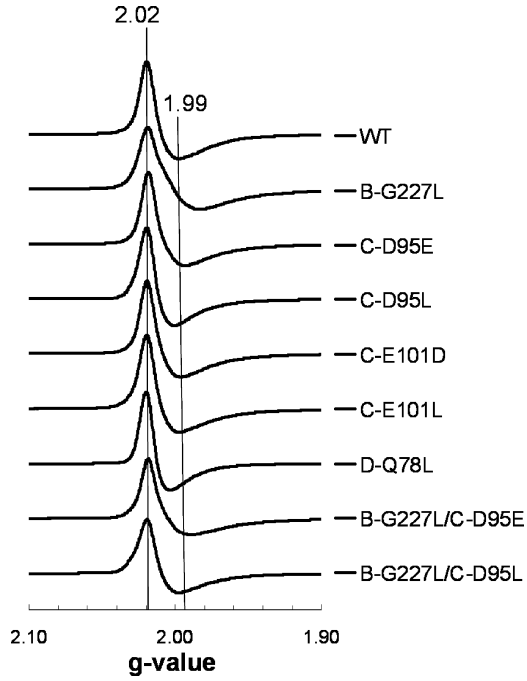

FIGURE 5: EPR spectra of the oxidized [3Fe-4S] cluster. Data were obtained under the following instrument conditions: temperature, 12 K; microwave power, 20 mW at 9.38 GHz; modulation amplitude, 10 G_{pp} at 100 KHz. Spectra were taken during redox titrations wherein the [3Fe-4S] cluster is fully oxidized (poised at +118 mV or higher). Each spectrum is collected from a 200 μL sample at approximately 30 mg mL^{-1} total protein concentration wherein the Sdh enzyme is present at approximately 2 nmol mg^{-1}.

We next determined the effects of the mutations on the EPR spectroscopic properties of the [3Fe-4S] cluster, which is in close proximity to the Q_P-site; Figure 5 shows the effects of the mutations on its EPR line shape. The SdhCDAB^{G227L} mutant exhibits a minor broadening of the oxidized [3Fe-4S] peak−trough signal wherein the peak remains at $g = 2.02$ and the trough shifts from $g = 1.99$ to $g = 1.98$. The SdhC^{D95E}DAB^{G227L} mutant, but not the SdhC^{D95L}DAB^{G227L} mutant, also experiences this broadening in the EPR line shape of its [3Fe-4S] cluster. The SdhCD^{Q78L}AB mutant shows an opposing effect where its trough is actually shifted from $g = 1.99$ to $g = 2.00$. Data from redox titrations suggest that only the SdhC^{D95L}DAB mutant has an effect on the midpoint potential of the [3Fe-4S] cluster, which is shifted modestly from +52 mV in the WT enzyme to +87 mV (Table 6).

With respect to the EPR spectrum of the heme, the WT Sdh enzyme exhibits a broad signal that comprises two

Table 6: Midpoint Potentials of [3Fe-4S] Cluster and Heme *b*[a]

mutant	[3Fe-4S] E_m (mV)	heme *b* E_m (mV)
WT	+52	+20
B-G227L	+60	−5
C-D95E	+56	−40
C-D95L	+87	+17
C-E101D	+51	+10
C-E101L	+55	+12
D-Q78L	+65	+8
B-G227L/C-D95E	+77	−10
B-G227L/C-D95L	+86	+42

[a] Two redox titrations on membrane preparations containing each Sdh construct were carried out at pH 7. Dithionite was used solely as a reductant in one titration (decreasing reduction potential) whereas ferricyanide was used solely as an oxidant in the other titration (increasing reduction potential). 200 μL samples poised at varying reduction potentials were frozen with liquid nitrogen-chilled ethanol and analyzed by EPR. Data were obtained under the following instrument conditions: temperatures, 12 K ([3Fe-4S] cluster) and 9 K (heme b); microwave power, 20 mW at 9.38 GHz; modulation amplitude, 10 G_{pp} at 100 KHz. The signal at $g = 2.02$ was used to determined the midpoint potential ($E_{m,7}$) of the [3Fe-4S] cluster while the $g = 3.66$ signal was used for the heme *b*. Data from the two titrations were merged, and the Nernst equation was fitted to obtain the $E_{m,7}$ value of each cofactor. The error in $E_{m,7}$ values is approximately ±10 mV.

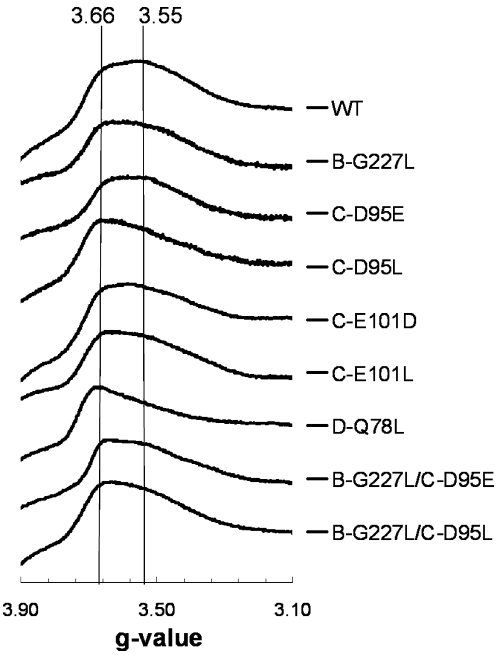

FIGURE 6: EPR spectra of the oxidized heme *b*. Three scans of each sample were taken to form each individual spectrum. Data were obtained under the following instrument conditions: temperature, 9 K; microwave power, 20 mW at 9.38 GHz; modulation amplitude, 10 G_{pp} at 100 KHz. Spectra were taken during redox titrations wherein the heme *b* is fully oxidized (poised at +117 mV or higher). Each spectrum is collected from a 200 μL sample at approximately 30 mg mL^{-1} total protein concentration wherein the Sdh enzyme is present at approximately 2 nmol mg^{-1}.

overlapping peaks located at $g = 3.66$ and $g = 3.55$. Some of the mutations presented herein appear to alter the relative intensities of these two peaks (Figure 6). SdhCDAB^{G227L}, SdhC^{D95L}DAB, SdhC^{E101L}DAB, and SdhCD^{Q78L}AB, as well as the two double mutants, are able to elicit an downfield shift of the low-spin heme signal toward the $g = 3.66$ species. Analyses on the heme *b* indicate that all mutations along the putative water channel cause a decrease in its E_m value with the exception of the double mutant SdhAB^{G227L}C^{D95L}D (Table 6).

DISCUSSION

In this study, we set out to determine if the water channel observed in the X-ray crystal structure of *E. coli* Sdh served as a H^+ delivery pathway from the cytoplasm to the Q_P-site (*1, 16*). Chains of electron densities interpreted to be water molecules are observed in the three known Sdh structures, but differences exist between the precise residues involved. In *E. coli* Sdh, the entrance to the proton pathway is surrounded by residues $SdhB^{G227}$ and $SdhC^{E101}$, with $SdhC^{D95}$ nearby (*1*); in the two mammalian complex II structures (Supporting Information Figures 1 and 2), the water molecule at the hydrophobic/hydrophilic interface interacts with the side chain of a glutamine residue that is equivalent to $SdhD^{Q78}$ in *E. coli* Sdh (*2, 3*). Furthermore, the number and positions of water molecules along the proton pathway differ significantly among the three structures. Thus the role of these four residues in enzyme catalysis was examined.

Our data clearly indicate that mutations surrounding the putative water channel have little effect on the ability of the enzyme to support aerobic respiratory growth on succinate but have a profound effect on anaerobic growth on glycerol−fumarate. At both pH 7 and pH 8, the Sdh mutant enzymes retained significant succinate:Q_0 oxidoreductase activity; thus their ability to sustain aerobic growth on succinate is not surprising. Given the high *in vitro* plumbagin:fumarate oxidoreductase activities observed in all the mutant enzymes, the variation of anaerobic growth rates on G-F minimal medium was unexpected. As the availability of ATP is limited during anaerobic growth on G-F, the poor growth rates of $SdhCDAB^{G227L}$, $SdhC^{D95L}DAB$, $SdhC^{E101L}DAB$, and the double mutants suggested that *in vivo* expression of the mutant enzymes was compromising the energy efficiency of the cells, possibly by making the membranes more permeable to H^+ and thereby destroying the protonmotive force. To rule out this possibility, we monitored anaerobic growth on minimal media where dimethyl sulfoxide was used as the terminal electron acceptor in place of fumarate (*34*). If the cells were leaky to H^+, this should lead to compromised growth as was shown in Figure 3B, but this was not observed (data not shown). We also found that whole cells expressing the various mutant enzymes did not show a higher rate of H^+ influx when exposed to an acid pulse (*41*). Thus the effects of the mutants examined herein appear to be specific to Sdh.

In D_2O, the mutant enzymes generally have similar rates of plumbagin oxidation but apparent decreased quinone reductase activities compared to the WT enzyme. This translates into a significantly larger KIE for the WT enzyme compared to the mutant enzymes in the plumbagin:fumarate assay, but not the succinate:Q_0 assay (Figure 4, Table 5). This implies that reversible proton transfer between the cytoplasm and the Q_P-site may be comprised of nonequivalent pathways using water molecules located at different locations. Specifically, there may be alternate water channels that are associated with different redox states of the heme (*42*). This latter explanation may account for the diversity and variation of the number and positions of the water molecules observed in the three crystal structures of Sdh.

In the kinetic data presented in Tables 3 and 4, two mutant enzymes stand out in particular: $SdhCDAB^{G227L}$, which had a significantly higher rate of Q_0 reduction at pH 8 compared to pH 7, and $SdhCD^{Q78L}AB$, which had higher k_{cat}/K_m values for the succinate:Q_0 reaction at pH 8 and the plumbagin:fumarate reaction at pH 7 relative to the WT enzyme. The altered kinetic properties of these two mutant enzymes are consistent with the fact that the two residues are located at the observed entrances to the membrane intrinsic water channel in the *E. coli* and eukaryotic Sdh structures, respectively. In an attempt to completely preclude solvent accessibility in the former enzyme, the double mutants $SdhC^{D95E}DAB^{G227L}$ and $SdhC^{D95L}DAB^{G227L}$ were created. Intriguingly, the $SdhC^{D95L}DAB^{G227L}$ mutant enzyme had a comparable rate of succinate-dependent Q_0 reduction as the WT enzyme but remained compromised in its ability to carry out fumarate-dependent plumbagin oxidation. As discussed above, both double mutant enzymes were unable to rescue anaerobic growth of DW35 on G-F despite retaining significant plumbagin:fumarate activity. To explain this apparent paradox, we propose that the *E. coli* Sdh uses an alternative water channel to transport protons to/from the cytoplasm from/to the Q_P-site when proton channel mutations close off the H^+ pathway. Examination of the *E. coli* Sdh structure revealed an alternative pathway for H^+ movement that involves residue $SdhD^{D15}$ and HOH45 (PDB file 1NEK). This pathway is not visible when the enzyme is viewed from the "side" (parallel to the membrane) but becomes apparent when viewed from the cytoplasm (Figure 7). Further, this pathway appears to be more efficient in that it involves only 5 ordered water molecules as opposed to a sequence of 13 water molecules which span the entire length of the protein as proposed by Horsefield et al. (*16*). Most importantly, the location of HOH45 is also equivalent to the positions at which the water channel entrance is located in the pig and chicken Sdh enzymes, finally bringing a sense of coherency among the three Sdh structures.

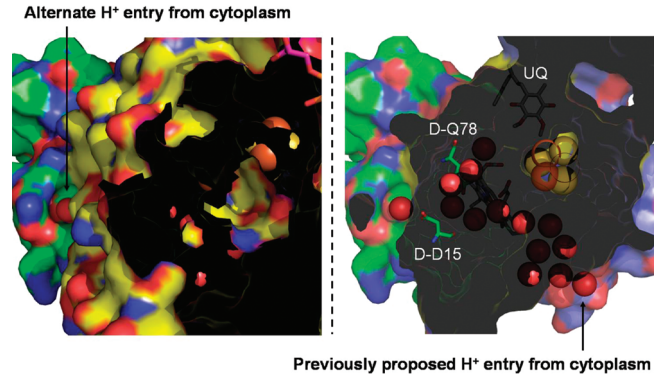

FIGURE 7: An alternative proton entry point in *E. coli* Sdh. Surface (left) and cut-away (right) perspectives of the observed water channel as viewed from SdhA toward the membrane. HOH45 in PDB file 1NEK can also serve as an entrance that brings protons from the cytoplasm to the Q_P-site. This proton pathway also involves residue $SdhD^{D15}$ and only involves five ordered water molecules. HOH45 also corresponds to the observed proton entry point in the pig and chicken Sdh structures. The figure was generated from PDB file 1NEK using PyMOL v.0.99 (DeLano Scientific LLC).

The existence of multiple proton channels in redox enzymes is not newfound and has been extensively studied most notably in the cytochrome oxidase family of enzymes and the bacterial photosynthetic reaction center. In cytochrome *c* oxidase, up to three possible proton pathways (D-, K-, and H-pathways) may facilitate proton translocation

across the energy conserving membrane. In a high-resolution crystal structure of the *Rhodobacter sphaeroides* reaction center, multiple water channels were observed to connect the Q_B molecule to the aqueous phase and converge at a key Asp residue near Q_B (*43, 44*). Single mutations of His-H126 and His-H128, residues located at the entrance to one of the water channels, did not affect proton uptake but double replacement of His with Ala impeded the rate of proton uptake by ~4−10-fold (*45*). The retention of proton uptake ability in the mutant reaction centers indicates other water channels are capable of proton conductance from the aqueous phase to the quinone molecule.

As our data suggest, the water channel entrance involving $SdhD^{D15}$ may only function *in vitro*, or is nonfunctional *in vivo* under anaerobic conditions. It is unclear why this may be the case, but one possible explanation involves the binding of menaquinol to the Q_P-site *in vivo*. With regard to the porcine Sdh enzyme, it was proposed that the hydrophobic tail of the UQ molecule wraps around the SdhCD domain such that it induces closure to the Q_D-site (*2*). In *E. coli* Sdh, it is conceivable by analogy that the isoprenoid tail of the quinone molecule can wrap around the membrane anchor domain such that the hydrophilic opening to the water channel via $SdhD^{D15}$ is blocked. Since plumbagin does not have any isoprenoid extensions, H^+ can enter/exit Sdh at $SdhD^{D15}$ even if the proton channel mutations studied herein close off the H^+ pathway further down the water chain. An alternate possibility to account for the discrepancy between the *in vivo* and *in vitro* activities is the presence of a weakly bound lipid that is washed off during enzyme preparation. Finally, the different oligomeric states of Sdh *in vivo* and *in vitro* could also account for the discrepancy since intersubunit contacts between neighboring Sdh could deny accessibility at the $SdhD^{D15}$ entrance. However, this last scenario is unlikely since we did not employ any detergents during our enzyme preparations and used isolated membranes in all our assays.

Studies on the proton channel were recently carried out in the heme-free Sdh mutants from *E. coli* (*6*) and *Saccharomyces cerevisiae* (*22*). In the crystal structure, one of the propionate groups of the heme *b* interacts with the water channel (*1*); removal of the heme would most likely bring disorder to the existing water molecules and perhaps even allow additional water molecules into the void normally occupied by the heme. The *E. coli* and *S. cerevisiae* heme-free enzymes maintain approximately 50−70% of its catalytic activity at pH 7, similar to the results observed in this study. Thus the Q_P-site appears to be relatively robust in that it can still carry out quinone reaction chemistry despite disruption of the water channel leading toward it, most likely because the final water molecule (HOH39) is still present and stabilized by residues $SdhB^{H207}$, $SdhC^{R31}$, and $SdhD^{D82}$ (*16*). Given the mutations studied herein affect the water channel, it is conceivable that some long-range effect might be propagated to the Q_P-site. However, apparent K_m values for Q_0 and plumbagin were only slightly affected in our enzyme assays. Furthermore, it is known that only an intact and functional Q_P-site can bridge electron transfer from the [3Fe-4S] cluster to the heme *b* (*21*). Since the heme cofactor is reducible by succinate in all mutant enzymes (data not shown), it can be inferred that binding and release of endogenous quinone/quinol molecules are not significantly affected.

Oyedotun and Lemire had previously examined the strictly conserved Sdh3p-D117 residue in *S. cerevisiae* Sdh and discovered a long-range translational effect on the flavin active site in the form of a *decreased* succinate:PMS turnover rate (*46*). In this study, a similar phenomenon was observed when the equivalent $SdhC^{D95}$ residue was substituted with a glutamate; however, the $SdhC^{D95E}DAB$ mutant, as well as the $SdhC^{D95E}DAB^{G227L}$ mutant, showed an *increase* in succinate:PMS/MTT turnover. Thus it appears that $SdhC^{D95}$, a residue that H-bonds to the water channel, has the ability to exert intersubunit control on the catalytic SdhAB dimer. Interestingly, the $SdhC^{D95E}DAB$ mutation also shifts the midpoint potential of the heme from +20 to −40 mV. To date, it remains uncertain what the exact function of the heme *b* is in Sdh. Clearly, it plays a role in enzyme stability, but it is not necessary for its assembly or for enzyme catalysis *in vitro* and *in vivo*, and it does not suppress generation of reactive oxygen species as some have suggested (*1, 6, 22*). Can it be that the heme acts as a redox sensor and communicates this information to the FAD site such that succinate oxidation and electron transfer are coupled to proton transfer and ubiquinone reduction?

Because the heme interacts with the water channel via H-bonds, spectroscopic data gathered on this cofactor would indicate whether its surroundings have been significantly altered. The reduced-*minus*-oxidized UV−visible spectra of the heme *b* in the mutant enzymes show no obvious deviation from that of the WT enzyme (data not shown). EPR analyses on the oxidized heme showed that the $SdhCDAB^{G227L}$, $SdhC^{D95L}DAB$, $SdhC^{E101L}DAB$, and $SdhCD^{Q78L}AB$ mutations cause a change in its EPR line shape, indicating an alteration in the local environment or the conformation of this prosthetic group. Note that this change in EPR line shape is not observed in the $SdhC^{D95E}DAB$ and $SdhC^{E101D}DAB$ mutant enzymes wherein the carboxylate side chains are maintained. Rothery et al. have carried out redox titrations and *in silico* simulations on the heme whereby a $SdhC^{H91L}DAB$ mutation shifts the EPR signal to the $g = 3.66$ species and a $SdhCD^{R20L}AB$ mutation shifts the EPR signal to the $g = 3.55$ species (unpublished data). It is believed that the two mutants alter the conformation of one of the propionate arms of the heme such that the H-bonding network involving the water channel is altered. All four leucine variants mentioned herein caused the equilibrium to shift toward the $g = 3.66$ species, indicating that they all had the same disruptive effect on the water channel.

With this work on the H^+ pathway and water channel, an understanding of the complexity underlying the workings of the succinate dehydrogenase enzyme is beginning to emerge. Mutational analyses of $SdhC^{D95}$ provide a glimpse of how proton transfer may be coupled to succinate oxidation and possibly electron transfer in the catalytic dimer. We found that disruption of the water channel near its entrance into the hydrophobic SdhCD domain slows down, but does not completely inhibit, catalysis. *In vivo* activity, but not *in vitro* activity, was significantly altered when the mutants were forced to function as a fumarate reductase. Based on the structures of the pig and chicken Sdh, as well as our data, we present an alternative proton pathway that only appears

to be functional *in vitro*. This pathway involves residue $SdhD^{D15}$, which appears to be a worthy candidate for future experiments.

SUPPORTING INFORMATION AVAILABLE

Figures 1 and 2 depict the ordered water molecules in porcine and chicken Sdh enzymes that lead from the aqueous phase to the quinone binding site. In both crystal structures, the entrance to the water channel is located at an Asp residue. This material is available free of charge via the Internet at http://pubs.acs.org.

REFERENCES

1. Yankovskaya, V., Horsefield, R., Tornroth, S., Luna-Chavez, C., Miyoshi, H., Leger, C., Byrne, B., Cecchini, G., and Iwata, S. (2003) Architecture of succinate dehydrogenase and reactive oxygen species generation. *Science 299*, 700–704.
2. Sun, F., Huo, X., Zhai, Y., Wang, A., Xu, J., Su, D., Bartlam, M., and Rao, Z. (2005) Crystal structure of mitochondrial respiratory membrane protein complex II. *Cell 121*, 1043–1057.
3. Huang, L. S., Sun, G., Cobessi, D., Wang, A. C., Shen, J. T., Tung, E. Y., Anderson, V. E., and Berry, E. A. (2006) 3-nitropropionic acid is a suicide inhibitor of mitochondrial respiration that, upon oxidation by complex II, forms a covalent adduct with a catalytic base arginine in the active site of the enzyme. *J. Biol. Chem. 281*, 5965–5972.
4. Reid, G. A., Miles, C. S., Moysey, R. K., Pankhurst, K. L., and Chapman, S. K. (2000) Catalysis in fumarate reductase. *Biochim. Biophys. Acta 1459*, 310–315.
5. Tomasiak, T. M., Maklashina, E., Cecchini, G., and Iverson, T. M. (2008) A threonine on the active site loop controls transition state formation in Escherichia coli respiratory complex II. *J. Biol. Chem. 283*, 15460–15468.
6. Tran, Q. M., Rothery, R. A., Maklashina, E., Cecchini, G., and Weiner, J. H. (2007) Escherichia coli succinate dehydrogenase variant lacking the heme b. *Proc. Natl. Acad. Sci. U.S.A. 104*, 18007–18012.
7. Iverson, T. M., Luna-Chavez, C., Cecchini, G., and Rees, D. C. (1999) Structure of the Escherichia coli fumarate reductase respiratory complex. *Science 284*, 1961–1966.
8. Oyedotun, K. S., and Lemire, B. D. (2001) The quinone-binding sites of the Saccharomyces cerevisiae succinate-ubiquinone oxidoreductase. *J. Biol. Chem. 276*, 16936–16943.
9. Iverson, T. M., Luna-Chavez, C., Croal, L. R., Cecchini, G., and Rees, D. C. (2002) Crystallographic studies of the Escherichia coli quinol-fumarate reductase with inhibitors bound to the quinol-binding site. *J. Biol. Chem. 277*, 16124–16130.
10. Cecchini, G., Maklashina, E., Yankovskaya, V., Iverson, T. M., and Iwata, S. (2003) Variation in proton donor/acceptor pathways in succinate:quinone oxidoreductases. *FEBS Lett. 545*, 31–38.
11. Schnorpfeil, M., Janausch, I. G., Biel, S., Kroger, A., and Unden, G. (2001) Generation of a proton potential by succinate dehydrogenase of Bacillus subtilis functioning as a fumarate reductase. *Eur. J. Biochem. 268*, 3069–3074.
12. Schirawski, J., and Unden, G. (1998) Menaquinone-dependent succinate dehydrogenase of bacteria catalyzes reversed electron transport driven by the proton potential. *Eur. J. Biochem. 257*, 210–215.
13. Madej, M. G., Nasiri, H. R., Hilgendorff, N. S., Schwalbe, H., Unden, G., and Lancaster, C. R. (2006) Experimental evidence for proton motive force-dependent catalysis by the diheme-containing succinate:menaquinone oxidoreductase from the Gram-positive bacterium Bacillus licheniformis. *Biochemistry 45*, 15049–15055.
14. Lancaster, C. R., Sauer, U. S., Gross, R., Haas, A. H., Graf, J., Schwalbe, H., Mantele, W., Simon, J., and Madej, M. G. (2005) Experimental support for the "E pathway hypothesis" of coupled transmembrane e^- and H^+ transfer in dihemic quinol:fumarate reductase. *Proc. Natl. Acad. Sci. U.S.A. 102*, 18860–18865.
15. Madej, M. G., Nasiri, H. R., Hilgendorff, N. S., Schwalbe, H., and Lancaster, C. R. (2006) Evidence for transmembrane proton transfer in a dihaem-containing membrane protein complex. *EMBO J. 25*, 4963–4970.
16. Horsefield, R., Yankovskaya, V., Sexton, G., Whittingham, W., Shiomi, K., Omura, S., Byrne, B., Cecchini, G., and Iwata, S. (2006) Structural and computational analysis of the quinone-binding site of complex II (succinate-ubiquinone oxidoreductase): a mechanism of electron transfer and proton conduction during ubiquinone reduction. *J. Biol. Chem. 281*, 7309–7316.
17. Maklashina, E., Iverson, T. M., Sher, Y., Kotlyar, V., Andrell, J., Mirza, O., Hudson, J. M., Armstrong, F. A., Rothery, R. A., Weiner, J. H., and Cecchini, G. (2006) Fumarate reductase and succinate oxidase activity of Escherichia coli complex II homologs are perturbed differently by mutation of the flavin binding domain. *J. Biol. Chem. 281*, 11357–11365.
18. Hudson, J. M., Heffron, K., Kotlyar, V., Sher, Y., Maklashina, E., Cecchini, G., and Armstrong, F. A. (2005) Electron transfer and catalytic control by the iron-sulfur clusters in a respiratory enzyme, E. coli fumarate reductase. *J. Am. Chem. Soc. 127*, 6977–6989.
19. Anderson, R. F., Hille, R., Shinde, S. S., and Cecchini, G. (2005) Electron transfer within complex II. Succinate:ubiquinone oxidoreductase of Escherichia coli. *J. Biol. Chem. 280*, 33331–33337.
20. Cheng, V. W., Ma, E., Zhao, Z., Rothery, R. A., and Weiner, J. H. (2006) The iron-sulfur clusters in Escherichia coli succinate dehydrogenase direct electron flow. *J. Biol. Chem. 281*, 27662–27668.
21. Tran, Q. M., Rothery, R. A., Maklashina, E., Cecchini, G., and Weiner, J. H. (2006) The quinone binding site in Escherichia coli succinate dehydrogenase is required for electron transfer to the heme b. *J. Biol. Chem. 281*, 32310–32317.
22. Oyedotun, K. S., Sit, C. S., and Lemire, B. D. (2007) The Saccharomyces cerevisiae succinate dehydrogenase does not require heme for ubiquinone reduction. *Biochim. Biophys. Acta 1767*, 1436–1445.
23. Zhao, Z., Rothery, R. A., and Weiner, J. H. (2006) Effects of site-directed mutations in Escherichia coli succinate dehydrogenase on the enzyme activity and production of superoxide radicals. *Biochem. Cell Biol. 84*, 1013–1021.
24. Szeto, S. S., Reinke, S. N., Sykes, B. D., and Lemire, B. D. (2007) Ubiquinone-binding site mutations in the Saccharomyces cerevisiae succinate dehydrogenase generate superoxide and lead to the accumulation of succinate. *J. Biol. Chem. 282*, 27518–27526.
25. Burgeois, M., Goutieres, F., Chretien, D., Rustin, P., Munnich, A., and Aicardi, J. (1992) Deficiency in complex II of the respiratory chain, presenting as a leukodystrophy in two sisters with Leigh syndrome. *Brain Dev. 14*, 404–408.
26. Horvath, R., Abicht, A., Holinski-Feder, E., Laner, A., Gempel, K., Prokisch, H., Lochmuller, H., Klopstock, T., and Jaksch, M. (2006) Leigh syndrome caused by mutations in the flavoprotein (Fp) subunit of succinate dehydrogenase (SDHA). *J. Neurol. Neurosurg. Psychiatry 77*, 74–76.
27. Rivner, M. H., Shamsnia, M., Swift, T. R., Trefz, J., Roesel, R. A., Carter, A. L., Yanamura, W., and Hommes, F. A. (1989) Kearns-Sayre syndrome and complex II deficiency. *Neurology 39*, 693–696.
28. Riggs, J. E., Schochet, S. S., Jr., Fakadej, A. V., Papadimitriou, A., DiMauro, S., Crosby, T. W., Gutmann, L., and Moxley, R. T. (1984) Mitochondrial encephalomyopathy with decreased succinate-cytochrome c reductase activity. *Neurology 34*, 48–53.
29. Arpa, J., Campos, Y., Gutierrez-Molina, M., Cruz-Martinez, A., Arenas, J., Caminero, A. B., Palomo, F., Morales, C., and Barreiro, P. (1994) Benign mitochondrial myopathy with decreased succinate cytochrome C reductase activity. *Acta Neurol. Scand. 90*, 281–284.
30. Favier, J., Briere, J. J., Strompf, L., Amar, L., Filali, M., Jeunemaitre, X., Rustin, P., and Gimenez-Roqueplo, A. P. (2005) Hereditary paraganglioma/pheochromocytoma and inherited succinate dehydrogenase deficiency. *Horm. Res. 63*, 171–179.
31. Westenberg, D. J., Gunsalus, R. P., Ackrell, B. A., Sices, H., and Cecchini, G. (1993) Escherichia coli fumarate reductase frdC and frdD mutants. Identification of amino acid residues involved in catalytic activity with quinones. *J. Biol. Chem. 268*, 815–822.
32. Maklashina, E., Berthold, D. A., and Cecchini, G. (1998) Anaerobic expression of Escherichia coli succinate dehydrogenase: functional replacement of fumarate reductase in the respiratory chain during anaerobic growth. *J. Bacteriol. 180*, 5989–5996.
33. Sambrook, J., and Russell, D. W. (2001) *Molecular cloning: a laboratory manual*, 3rd ed., Cold Spring Harbor Laboratory Press, Cold Spring Harbor, NY.

34. Sambasivarao, D., and Weiner, J. H. (1991) Dimethyl sulfoxide reductase of Escherichia coli: an investigation of function and assembly by use of in vivo complementation. *J. Bacteriol. 173*, 5935–5943.
35. Lowry, O. H., Rosebrough, N. J., Farr, A. L., and Randall, R. J. (1951) Protein measurement with the Folin phenol reagent. *J. Biol. Chem. 193*, 265–275.
36. Markwell, M. A., Haas, S. M., Bieber, L. L., and Tolbert, N. E. (1978) A modification of the Lowry procedure to simplify protein determination in membrane and lipoprotein samples. *Anal. Biochem. 87*, 206–210.
37. Singer, T. P., and Edmondson, D. E. (1980) Structure, properties, and determination of covalently bound flavins. *Methods Enzymol. 66*, 253–264.
38. Kita, K., Vibat, C. R., Meinhardt, S., Guest, J. R., and Gennis, R. B. (1989) One-step purification from Escherichia coli of complex II (succinate: ubiquinone oxidoreductase) associated with succinate-reducible cytochrome b556. *J. Biol. Chem. 264*, 2672–2677.
39. Maklashina, E., and Cecchini, G. (1999) Comparison of catalytic activity and inhibitors of quinone reactions of succinate dehydrogenase (Succinate-ubiquinone oxidoreductase) and fumarate reductase (Menaquinol-fumarate oxidoreductase) from Escherichia coli. *Arch. Biochem. Biophys. 369*, 223–232.
40. Cleland, W. W. (2005) The use of isotope effects to determine enzyme mechanisms. *Arch. Biochem. Biophys. 433*, 2–12.
41. King, S. C., and Wilson, T. H. (1990) Characterization of Escherichia coli lactose carrier mutants that transport protons without a cosubstrate. Probes for the energy barrier to uncoupled transport. *J. Biol. Chem. 265*, 9645–9651.
42. Berghuis, A. M., and Brayer, G. D. (1992) Oxidation state-dependent conformational changes in cytochrome c. *J. Mol. Biol. 223*, 959–976.
43. Stowell, M. H., McPhillips, T. M., Rees, D. C., Soltis, S. M., Abresch, E., and Feher, G. (1997) Light-induced structural changes in photosynthetic reaction center: implications for mechanism of electron-proton transfer. *Science 276*, 812–816.
44. Abresch, E., Paddock, M. L., Stowell, M. H., McPhillips, T. M., Axelrod, H. L., Soltis, S. M., Rees, D. C., Okamura, M. Y., and Feher, G. (1998) Identification of proton transfer pathways in the X-ray crystal structure of the bacterial reaction center from Rhodobacter sphaeroides. *Photosyn. Res. 55*, 119–125.
45. Adelroth, P., Paddock, M. L., Tehrani, A., Beatty, J. T., Feher, G., and Okamura, M. Y. (2001) Identification of the proton pathway in bacterial reaction centers: decrease of proton transfer rate by mutation of surface histidines at H126 and H128 and chemical rescue by imidazole identifies the initial proton donors. *Biochemistry 40*, 14538–14546.
46. Oyedotun, K. S., and Lemire, B. D. (1999) The Saccharomyces cerevisiae succinate-ubiquinone oxidoreductase. Identification of Sdh3p amino acid residues involved in ubiquinone binding. *J. Biol. Chem. 274*, 23956–23962.

BI801008E